PHYSICAL REVIEW B VOLUME 45, NUMBER 23 15 JUNE 1992-I

Photoemission study of the surface electronic structure of Mo(001) and Mo(001)-2H

Kevin E. Smith* and Stephen D. Kevan
Department of Physics, University of Oregon, Eugene, Oregon 97403

(Received 3 February 1992)

We report a high-resolution angle-resolved photoemission study of the surface electronic structure of the room-temperature phase of Mo(001) and Mo(001)-2H. We have focused particularly upon the electron states on the clean surface within a few electron volts of the Fermi level in an attempt to characterize the interplay between the electronic and atomic structures of this surface. We relate these measurements of the surface band structure along the high-symmetry directions to recently published surface Fermi contours. Most importantly, we observe a band to be located at or near the Fermi level over a small region of momentum space, near the middle of the Σ line. This feature is well placed to couple to phonon modes characteristic of the low-temperature reconstruction observed on this surface. The relationship of these results to existing calculations, to our previous results for W(001), to the wave vector of the reconstruction, and to recent measurements of surface phonon dispersion relations will be discussed.

I. INTRODUCTION

Understanding the combination of forces which together cause the atoms at a crystal surface to move from their bulk lattice positions (surface reconstruction) has provided an enduring focus of surface physics. Prototypical clean-surface reconstructions are observed on W(001) (Ref. 1) and Mo(001) (Ref. 2) below room temperature, which form $c(2\times2)$ and $(7\sqrt{2}\times\sqrt{2})R45°$ structures,[3,4] respectively. While the W(001) surface has been extensively studied both by computations and by a variety of surface techniques,[5] much less detailed information is available concerning Mo(001).[6-15] The local geometric arrangement of the surface atoms is thought to be similar on the two surfaces, i.e., zigzag chains of atoms oriented along the [110] azimuthal direction.[2-4] Thus the reconstructive mechanisms on the two surfaces are surely related. However, the difference in unit cell size is indicative of the difficulty of attaining a general understanding of this mechanism. Competing paradigmatic theories of the driving force for these reconstructions have been based upon mechanisms involving either a Peierls distortion[6,16] or the formation of localized bonds between surface atoms.[17] Recent computational[10,18,19] and experimental[5,7,20] work has demonstrated that the ground state for these surfaces must result from a delicate interplay between localized and delocalized electronic interactions.

In order to make a detailed comparison between these two structurally similar surfaces, we report here a complete experimental determination of the surface quasiparticle band structure for the room-temperature phases of Mo(001) and Mo(001)-2H using angle-resolved photoemission (ARP). The results for clean Mo(001) exhibit intriguing similarities to and differences from our previous results for W(001).[5] The results along $\bar{\Sigma}$ can be interpreted in qualitatively similar fashion to those for W(001). Specifically, we find a nearly nondespersive band very close to E_F, roughly 40% of the way from $\bar{\Gamma}$ to $\bar{M}$. In both systems, this band provides a simple unification of the localized and delocalized paradigms for the reconstruction. However, the degree of momentum-space localization is measured to be larger in Mo(001) than that on W(001). We conclude that the contribution from spatially delocalized forces is relatively more important in Mo(001) than on W(001). Along $\bar{\Delta}$ the surface bands of Mo(001) are very different from those of W(001), particularly near E_F. Also unlike W(001), we find that existing calculations of the surface electronic structure of the ideal unreconstructed Mo(001) surface provide a reasonably good first-order description of our experimental bands, at least for bands near E_F at momenta which are not strongly perturbed by the pseudopotential of the reconstruction superlattice.[10-13] The reduced magnitude of the spin-orbit interaction in the 4d metal may partially explain the relative success of calculations for Mo(001).

The format of this paper is as follows. The next section explains our experimental procedures. Section III presents our experimental results, and Sec. IV discusses their relation to existing calculations and to the clean-surface reconstructions. We summarize our conclusions in the final section.

II. EXPERIMENTAL PROCEDURES

These ARP experiments were performed at the National Synchrotron Light Source at Brookhaven National Laboratory, using light from the 750-MeV vacuum ultraviolet storage ring, a 6-m toroidal grating monochromator,[21] and a high-resolution angle-resolving electron spectrometer which has been described previously.[22] For these experiments, the total instrumental resolution was always less than 100 meV full width at half maximum, and the full angular acceptance was 1° or better. A single spectrum could be accumulated with adequate signal-to-noise ratio under these conditions in typically 2–5 min.

A molybdenum crystal 8 mm × 8 mm × 1 mm in size was oriented along the [001] bulk crystalline axis by Laue backreflection to within 0.5°. The sample was heated by electron bombardment of its rear surface, and the front surface temperature was measured with an optical pyrometer. Cleaning was achieved *in vacuo* by repetitive cycles of oxidation at 1400 K in 5×10^{-8} Torr of O_2 followed by flashing to 2300 K every few minutes. The base operating pressure of $0.8-1.2\times10^{-10}$ Torr was sufficient to maintain a clean surface for 15–20 min, as determined by the gradual disappearance of some of the more contamination-sensitive features in our photoemission spectra. These features were easily restored by thermally desorbing the residual hydrogen and carbon monoxide from the surface, which in practice was done after taking 2–3 spectra. This desorption procedure could be performed repeatedly for several days without degradation of the surface. The hydrogen-saturated surface was prepared by exposing the room-temperature surface to hydrogen gas in the form of H_2, either by backfilling the chamber or by placing the sample in the line of sight of a channel-plate array doser.

III. RESULTS AND DISCUSSION

Figure 1 shows several ARP spectra collected in the $\bar{\Delta}$ azimuth as a function of emission angle from the clean and hydrogen-saturated surfaces. The photon energy was 20 eV and the light incidence and polarization vectors were in the [100] mirror plane. This polarization probes states of even symmetry, ignoring the spin-orbit interaction. In this azimuthal direction, there are two features observed on the clean surface which are quenched upon adsorption of hydrogen. At normal emission, these are located at binding energies of 0.3 and 3.6 eV relative to the Fermi level (E_F), and have been characterized previously as surface states or resonances.[23] Our work confirms this assignment. The feature at lower binding energy is prominant at all energies measured, and exhibits very little dispersion with momentum normal to the surface. The lower, being of nominally even mirror plane symmetry in both mirror planes, is a strongly coupled surface resonance along $\bar{\Delta}$ since it is degenerate with the projection of the second even bulk band. The surface band is not clearly visible in Fig. 1 at $h\nu=20$ eV near normal emission, but is readily apparent at $h\nu=40$ eV. It is easily seen in Fig. 1 at parallel momenta near the surface Brillouin zone (SBZ) boundary, but exhibits substantial dispersion with normal momentum. This is indicated by the nondegeneracy of the experimental points in Fig. 2 at 20 and 40 eV photon energy.

Both of these surface features are quenched upon hydrogen adsorption, and two features appear which are characteristic of the hydrogen-saturated surface. One of these is observed very close to E_F over much of the SBZ. This feature was discussed previously in detail regarding damping of adsorbate vibrations.[9,15] A second feature on

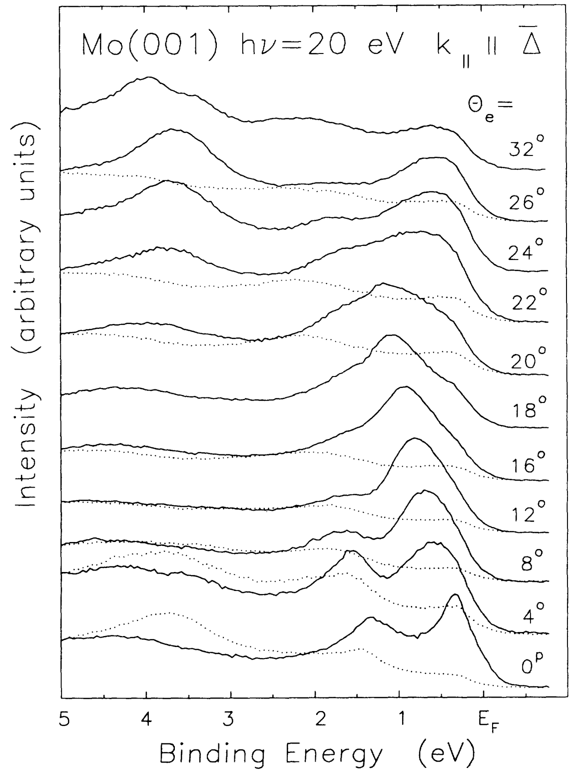

FIG. 1. ARP spectra of clean (solid curves) and hydrogen-covered (dashed curves) Mo(001) collected with the electron emission direction and the photon polarization vector in the same $\bar{\Delta}$ mirror plane, at a photon energy of 20 eV, as a function of emission angle measured from the sample normal. At this energy, the $\bar{X}$ symmetry point at the Fermi level is sampled at an emission angle of 34°.

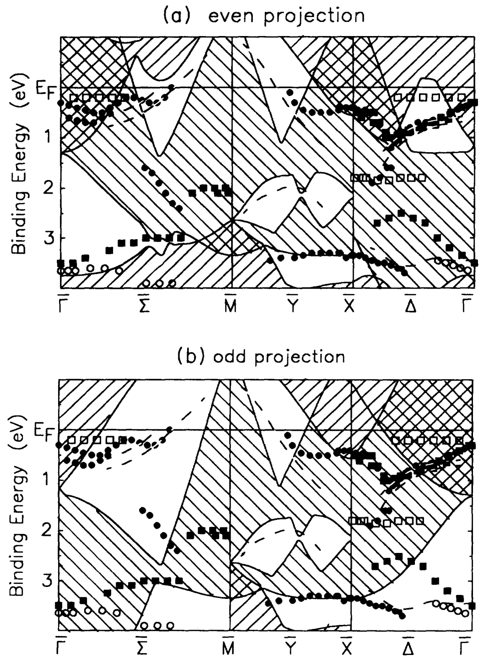

FIG. 2. Experimental dispersion relations of the surface-localized states on clean and hydrogen-covered Mo(001). Solid (open) symbols refer to the clean (hydrogen-covered) surfaces, respectively, while circles (squares) correspond to data collected at 20 eV (40 eV) photon energy. The shaded regions correspond to the projection of the bulk molybdenum band structure onto the (001) surface Brillouin zone, with for each band separately crosshatched. The calculation does not include the spin-orbit interaction, and panels (a) and (b) give the even and odd band projections within the two mirror-symmetry planes.

the hydrogen-saturated surface is localized near the zone boundary at roughly 2 eV binding energy and apparently has not previously been observed. The highest binding-energy feature on the hydrogen saturated surface is apparent in the spectra near normal emission in Fig. 1. It appears in Fig. 2 to be nearly degenerate with the low-lying clean-surface band. At intermediate coverages no corresponding hydrogen-induced feature is observed at this energy.

These data, coupled to similar results for the other symmetry lines in the SBZ, allow determination of the surface band dispersion relations shown graphically in Fig. 2. In this figure, the solid and open symbols refer to features observed on the clean and hydrogen-saturated surfaces, respectively. Symbols with different shapes correspond to the different photon energies given in the caption. The shaded regions in Figs. 2(a) and 2(b) correspond, respectively, to the projection of the even and odd calculated bulk band structures onto the (001) SBZ.[24] There is some uncertainty in comparing a calculated bulk band projection to our surface bands.[25] However, the calculation reproduces the measured bulk Fermi surface[26] very well, so that, at least near E_F, these projections provide a very good representation of reality.

The clean-surface bands near E_F along $\overline{\Sigma}$ have been discussed previously[14] in relation to the observed reconstruction. There is a doublet of bands within 1 eV of E_F which exhibit dispersion relations similar to those observed on W(001), except that the initial dispersion near Γ is clearly downward on Mo(001), while the dispersion is slowly upward on W(001).[5] As is the case for W(001), these two surface bands are presumably associated with projected gaps of odd and even symmetry which overlap significantly in this azimuth. The upper of the two surface bands disperses very close to E_F between $k_{\parallel}=0.54$ and 0.61 Å^{-1}. This band is well placed to contribute to the driving force for the reconstruction. In other words, the wave vector coupling this band with its image on the opposite side of the SBZ (1.1–1.2 Å^{-1}) is very close to the wave vector characterizing the $(7\sqrt{2}\times\sqrt{2})R45°$ structure and to the position of an anomaly in the surface phonon dispersion relations.[7] A connection to the driving force for the reconstruction was thereby deduced.[14] The second band of this doublet simply splits downward from the first away from zone center, only to merge with it further out in the zone. It is not possible to determine whether one of these two bands crosses E_F near the middle of the SBZ. Further out along $\overline{M}$, a single surface band crosses E_F along both the $\overline{\Sigma}$ and $\overline{Y}$ azimuths, thereby mimicking the behavior of the projected gap of even symmetry. These crossings form a well-defined hole pocket in the Fermi contours centered at $\overline{M}$.[14]

The dispersion relations of the two more tightly bound clean-surface bands along $\overline{\Sigma}$ on Mo(001) are quite similar to those observed on W(001).[5] One of these is located in a projected gap of even symmetry centered at the $\overline{\Gamma}$ point. Its dispersion relation follows that of the lower edge of this gap. The surface band observed near $\overline{M}$ is less clearly associated with any particular gap, although part of its dispersion does parallel the bottom of a large odd-symmetry gap.

Unlike the above results for the $\overline{\Sigma}$ and $\overline{Y}$ azimuths, the surface bands along $\overline{\Delta}$ for clean Mo(001) exhibit marked differences from those on W(001). The spectra in Fig. 1 exhibit one surface band near E_F, although we cannot rule out the possibility that two unresolved bands exist, as suggested in existing calculations (see below). This band disperses downwards across most of the azimuth, and reverses direction only near $\overline{X}$. While the observed band may be associated with the projected band gap of even symmetry in Fig. 2(a), it clearly disperses outside this gap without any significant change in intensity or shape. Unlike the corresponding band on W(001), this band never crosses E_F and there are thus no Fermi contours crossing this azimuth.[14] Taken in the context of all of our recent results on the (001) (Refs. 14 and 19) and (011) (Ref. 27) surfaces of Mo and W, this observation is surprising. In all cases except near $\overline{X}$ on Mo(001), there is a surface Fermi contour associated with the projection of the ellipsoidal segment of the bulk W and Mo Fermi surfaces onto the corresponding SBZ. For example, the projection of this ellipsoid is apparent near $\overline{M}$ in Fig. 2(a), and there is a surface contour which encloses this projection. The ellipsoid also projects about $\overline{X}$, but no surface orbit is observed. The fact that the clean-surface band near E_F disperses downward on Mo(001) along $\overline{\Delta}$ results in an exception to what appeared to be a general rule.

IV. RELEVANCE TO THE CLEAN-SURFACE RECONSTRUCTIONS

The bands calculated for the (1×1) unreconstructed surface[13] reproduced in Fig. 2 provide a remarkably good match to many of our experimental bands. This is particularly true for several bands near E_F, where the comparison between the calculated and measured bands is most appropriate.[25] For example, the calculation predicts bands crossing E_F near $\overline{M}$ along $\overline{\Sigma}$ and $\overline{Y}$ in close accord to our observations. The size of the hole pocket centered at $\overline{M}$ is thus accurately predicted by the calculation. All calculations significantly overestimate the size of the corresponding hole pocket on W(001).[5,19] The Fermi velocities of the calculated bands on Mo(001) are also quite close to the experimental values. The calculation also predicts two closely separated nearly parallel bands along $\overline{\Delta}$ close to E_F. The dispersion relations for these two bands nearly match our measured band, except that the calculated bands vanish before reaching zone center. Given that we can just barely resolve two shallow bands along $\overline{\Sigma}$, it is reasonable to suppose that our measured band along $\overline{\Delta}$ does indeed correspond to the calculated doublet.

A calculation of the (1×1) surface electronic structure thus produces bands in close accord with those measured for the room-temperature disordered or incommensurate surface. A likely reason for this is that the bands which are well produced in the calculation are not separated by wave vectors close to that of the reconstruction. In this case, the dispersion relations might be expected not to be strongly perturbed by the presence of the superlattice, rendering experimental bands fairly close to those of the (1×1) surface. In this sense, the pseudopotential of the superlattice is relatively weak compared to a typical bandwidth for the (1×1) surface.

An important discrepancy between our experimental and the calculated bands exists near the middle of the $\bar{\Sigma}$ line near E_F. The calculation predicts a doublet of monotonically upward-dispersing bands.[13] Neither of these bands reaches the zone center and both cross E_F at well-defined momenta along $\bar{\Sigma}$. At least one of our bands clearly does extend to zone center, and the dispersion relations are far from monotonic. The main deviations of the experimental from the calculated bands exist where the upper band is very close to E_F. As mentioned above, these regions are coupled by a wave vector very close to that of the reconstruction. The bands in this vicinity will thus be strongly perturbed by the pseudopotential associated with the reconstruction. Indeed, the observation that the agreement between experiment and theory is best at momenta removed from the middle of the $\bar{\Sigma}$ suggests very strongly that the deviations in this region are simply related to the reconstruction itself, and that these bands are intimately involved in driving the reconstruction.

The deviations of the experimental room-temperature bands from the calculated (1×1) bands are seen to be rather localized to the middle of the $\bar{\Sigma}$ line for Mo(001), while the deviations were observed to be extended through more of the SBZ on W(001).[5] That the deviations are "localized" in momentum space for Mo(001) suggests that the driving force for the reconstruction on this surface is fairly delocalized in real space, at least by comparison to W(001). In this sense, our results suggest that the charge-density-wave mechanism[6,16] is relatively more appropriate for Mo(001) than for W(001). This is to be expected, since the W($5d$) orbitals are more spatially extended than the Mo($4d$) orbitals, so that local bonding reconstruction mechanisms are relatively favored in the $5d$ metal. This speculation also fits the observation that the unit cell of the reconstruction on Mo(001) is much larger than that on W(001), and that the magnitude of the lateral atomic displacements on Mo(001) (Ref. 3) is measured to be smaller than that on W(001).[28] An energetic balance in favor of a spatially delocalized mechanism should optimize the unit cell dimension to couple segments of the Fermi contours precisely. Conversely, a balance in favor of a spatially localized mechanism will result in reconstruction into a smaller unit cell with a wave vector which may not be precisely associated with a vector coupling segments of the Fermi contours.

V. SUMMARY AND CONCLUSIONS

We have described a high-resolution angle-resolved photoemission study of the surface electronic structure of the room-temperature phase of clean Mo(001) and also of Mo(001)-2H. Our results exhibit some similarities to previous results on W(001), but also some important differences which we used to infer the relative importance of localized versus delocalized electronic mechanisms driving these surfaces to reconstruct. Our experimental bands are generally well reproduced by existing calculations, except in regions of the SBZ where the bands are strongly perturbed by the pseudopotential of the reconstruction superlattice.

ACKNOWLEDGMENTS

This work was carried out in part at the NSLS at Brookhaven National Laboratory, which is supported by the U.S. Department of Energy, Division of Materials Science and Division of Chemical Sciences. Financial support was received from the U.S. DOE under Grant No. DE-FG06-86ER45275. S.D.K. gratefully acknowledges partial support from the NSF and the A.P. Sloan Foundation.

---

[*] Present address: Physics Department, Boston University, Boston, MA 02215.

[1] M. K. Debe and D. A. King, Phys. Rev. Lett. **39**, 708 (1977); J. Phys. C **10**, L303 (1977); Surf. Sci. **81**, 193 (1979); J. Phys. C **15**, 2257 (1982).

[2] T. E. Felter, R. A. Barker, and P. J. Estrup, Phys. Rev. Lett. **38**, 1138 (1977); R. A. Barker, P. J. Estrup, F. Jona, and P. M. Marcus, Solid State Commun. **25**, 375 (1978).

[3] T. Felter, J. Vac. Sci. Technol A **2**, 1008 (1984); M. L. Hildner, R. S. Daley, T. E. Felter, and P. J. Estrup, *ibid.* **9**, 1604 (1991).

[4] D.-M. Smilgies and E. Hulpke, Phys. Rev. B **43**, 1260 (1991).

[5] For a review, see G. S. Elliott, K. E. Smith, and S. D. Kevan, Phys. Rev. B **44**, 10 826 (1991).

[6] J. E. Inglesfield, J. Phys. C **11**, L69 (1978).

[7] E. Hulpke and D.-M. Smilgies, Phys. Rev. B **40**, 1338 (1991).

[8] R. A. Barker, S. Semancik, and P. J. Estrup, Surf. Sci. **94**, L162 (1980).

[9] J. E. Reutt, Y. J. Chabal, and S. B. Christman, Phys. Rev. B **38**, 3112 (1988).

[10] X. W. Wang, C. T. Chan, K. M. Ho, and W. Weber, Phys. Rev. Lett. **60**, 2066 (1988).

[11] C. M. Bertoni, C. Calandra, and F. Manghi, Solid State Commun. **23**, 255 (1977).

[12] P. C. Stephenson and D. W. Bullett, Surf. Sci. **139**, 1 (1984).

[13] G. P. Kerker, K. M. Ho, and M. L. Cohen, Phys. Rev. Lett. **40**, 1593 (1978).

[14] K. E. Smith and S. D. Kevan, Phys. Rev. B **43**, 3986 (1991).

[15] K. E. Smith and S. D. Kevan, Phys. Rev. B **43**, 1831 (1991).

[16] E. Tosatti, Solid State Commun. **25**, 637 (1978); A. Fasolino, G. Santoro, and E. Tosatti, Phys. Rev. Lett. **44**, 1684 (1980); C. Z. Wang, A. Fasolino, and E. Tosatti, Surf. Sci. **211-212**, 323 (1989); H. Krakauer, M. Posternak, and A. J. Freeman, Phys. Rev. Lett. **43**, 1885 (1979).

[17] J. E. Inglesfield, J. Phys. C **12**, 149 (1979); K. Terakura, I. Terakura, and Y. Teraoka, Surf. Sci. **103**, 103 (1981); I. Terakura, K. Terakura, and N. Hamada, *ibid.* **111**, 479 (1981); J. C. Campuzano, D. A. King, C. Somerton, and J. E. Inglesfield, Phys. Rev. Lett. **45**, 1649 (1980); J. C. Campuzano, J. E. Inglesfield, D. A. King, and C. Somerton, J. Phys. C **14**, 3099 (1981); D. Singh and H. Krakauer, Phys. Rev. B **37**, 3999 (1988).

[18] W. K. Han and S. C. Ying, Phys. Rev. B **41**, 4403 (1990); **41**, 9163 (1990); T. L. Reinecke and S. C. Ying, *ibid.* **43**, 12 234 (1991).

[19] R. Yu, H. Krakauer, and D. Singh, Phys. Rev. B **45**, 9091

(1992).

[20]B. Salanon and J. Lapoujoulade, Surf. Sci. **173**, L613 (1983); H.-J. Ernst, E. Hulpke, and J. P. Toennies, Phys. Rev. Lett. **58**, 1941 (1987); Europhys. Lett. **10**, 747 (1989).

[21]P. Thiry, P. A. Bennett, S. D. Kevan, W. A. Royer, E. E. Chaban, J. E. Rowe, and N. V. Smith, Nucl. Instrum. Methods **222**, 85 (1984).

[22]S. D. Kevan, Rev. Sci. Instrum. **54**, 1441 (1983).

[23]S. L. Weng, E. W. Plummer, and T. Gustaffson, Phys. Rev. B **18**, 1718 (1978); S. L. Weng, T. Gustaffson, and E. W. Plummer, Phys. Rev. Lett. **44**, 344 (1980).

[24]D. A. Papaconstantopoulos, *Handbook of the Band Structure of Elemental Solids* (Plenum, New York, 1986).

[25]M. S. Hybertson and S. G. Louie, Phys. Rev. Lett. **55**, 1418 (1985); Phys. Rev. B **34**, 5390 (1986).

[26]D. M. Sparlin and J. A. Marcus, Phys. Rev. **144**, 484 (1966).

[27]R. H. Gaylord, K. Jeong, and S. D. Kevan, Phys. Rev. Lett. **62**, 2036 (1989); K. Jeong, R. H. Gaylord, and S. D. Kevan, Phys. Rev. B **39**, 2973 (1989); R. H. Gaylord, K. Jeong, S. Dhar, and S. D. Kevan, J. Vac Sci. Technol. A **7**, 2203 (1989).

[28]I. Stensgaard, L. C. Feldman, and P. J. Silverman, Phys. Rev. Lett. **42**, 247 (1979); I. Stensgaard, G. Purcell, and D. A. King, Phys. Rev. B **39**, 897 (1989); M. S. Altman, P. J. Estrup, and I. K. Robinson, *ibid.* **38**, 5211 (1988).